Original Article

Mechanical properties and ballistic behavior of LiF-added Al_2O_3–4 wt%Nb_2O_5 ceramics☆

Jheison Lopes dos Santos [a],*, Rubens Lincoln Santana Blazutti Marçal [a],
Paulo Roberto Rodrigues de Jesus [a], Alaelson Vieira Gomes [a], Édio Pereira Lima Jr [a],
Daniel Navarro da Rocha [a], Maria Aparecida Pinheiro dos Santos [b],
Lucio Fabio Cassiano Nascimento [a], Sergio Neves Monteiro [a], Luis Henrique Leme Louro [a]

[a] Military Institute of Engineering – IME, Department of Materials Science, Praça General Tibúrcio 80, Urca, 22290-270 Rio de Janeiro, RJ, Brazil
[b] Brazilian Navy Research Institute – IPqM, Division of Strucural and Electronic Ceramics, Rua Ipiru, 02, Cacuia, 21931-095 Rio de Janeiro, RJ, Brazil

ARTICLE INFO

ABSTRACT

For the first time, the behavior of LiF-added alumina-niobia ceramics was quasi-static and dynamically analyzed in ballistic tests. Different compositions were investigated for the compound Al_2O_3–4 wt%Nb_2O_5–nLiF, with n ranging from 0 to 1.50 wt%, processed at three different sintering temperatures (1300, 1350 and 1400 °C). Elastic properties, elastic wave velocities, Vickers microhardness and ballistic tests were performed according to standards. The results showed that the LiF addition benefits the Al_2O_3–4 wt%Nb_2O_5 ceramic properties, allowing to reduce by approximately 100 °C the sintering temperature without impairing the ballistic performance. The Al_2O_3–4 wt%Nb_2O_5–0.5 wt%LiF ceramics exhibit comparable properties to the commonly used Al_2O_3–4 wt%Nb_2O_5 ceramics.

1. Introduction

Aluminum oxide, or alumina (Al_2O_3), one important and most used engineering ceramics is fragile due to both low fracture strength and low tenacity [1–4]. The introduction of a second-phase reinforcement combined with sintering additives and annealing induced phase transformation, significantly improve the fracture strength and toughness of alumina-based ceramics, as well as alumina composites [5–9].

Aiming to improve the processing of alumina-based ceramics, Gomes et al. [10] reduced the sintering temperature by adding different fractions of niobium oxide, or niobia (Nb_2O_5). Their results indicated that even an addition of 4 wt% of

---

Nb_2O_5 in the alumina allowed the sintering temperature of the ceramic to be reduced from 1600 °C to 1450 °C, still maintaining its dynamic behavior, such as the ballistic protective capacity.

Lithium fluoride (LiF) has also been shown to be a potential sintering additive [11–14]. Indeed, highly dense MgO/Al_2O_3 spinels, with small additions of LiF, have been sintered as transparent ceramics [11,12]. Investigations [11–13] indicated that the LiF contribution is due to particle rearrangement, by formation of a transient liquid phase. Moreover, partial reactions yield oxygen lattice vacancies, promoting diffusion enhanced sintering [13]. Santos et al. [14] added LiF to the Al_2O_3–4 wt%Nb_2O_5 ceramic compound, to further reduce the sintering temperature. They optimized the addition of LiF by 0.5 wt%, obtaining about 90% of theoretical densification at just 1300 °C.

Due to its high compressive strength and hardness, an alumina-based ceramics may also be used as the front component in ballistic multilayered armor systems [15–18]. Its main function is to dissipate part of the projectile impact energy through the fragmentation of both the projectile tip as well as the front ceramic layer [15–19]. The second layer, just behind the ceramic, may be a high strength synthetic polymer fiber, such as aramid, or composites of polymeric matrix and natural fibers. The function of this layer is to retain fragments generated from the first layer of brittle material, as well as to assist in the partial dissipation of projectile energy [20–28].

The understanding of these mechanisms of fragmentation of the projectile and front ceramic, as well as capture of fragments by the second layer, relies on the comprehension of the dynamic behavior during the ballistic test. This behavior has been explained in terms of shock waves propagation inside a multilayered system [29]. The projectile impact energy dissipation depends on the resulting shock wave reflection at the interface between distinct layers. A greater energy dissipation occurs in case the second layer has a density lower than that of the front ceramic [23]. This is the case of aramid fiber, which is less dense than alumina-based ceramic investigated in a previous work [27]. The projectile-impacted compression shock wave is reflected at the interface as a tension shock wave, which contributes to an effective ceramic fragmentation associated with higher energy dissipation [27]

The present work investigates, for the first time, mechanical properties and ballistic behavior of LiF-added Al_2O_3–4 wt%Nb_2O_5 ceramic compounds. Microhardness values were measured for the LiF additions by weight of 0.25, 0.50, 0.75, 1.00, 1.25 and 1.50%. Subsequently, the elastic properties and wave velocities were determined for the addition of LiF optimized by Santos et al. [14]. In addition, this new 0.5 wt% LiF ceramic as well as a control LiF-free ceramic were ballistic tested as front layer followed by a Kevlar[TM] as second layer and Al alloy as back layer against high impact class III [30] 7.62 mm ammunition. The absorbed energy by the ceramic alone and the depth of penetration by the multilayered (ceramic/Kevlar[TM]/Al alloy) system were evaluated in corresponding ballistic tests against 7.62 projectiles.

2. Materials and methods

The precursor ceramic mixture, made in deionized water, was composed of 94.53 wt% alumina (Treibacher Schleifmittel, Brazil) and 3.94 wt% niobium oxide (CBMM, Brazil) together with polyethylene glycol, PEG, organic binder (1.53 wt%, from VETEC, Brazil). After the binder burnout, the ratio becomes Al_2O_3–4 wt%Nb_2O_5. Different additions of pro-analysis lithium fluoride (LiF, Vetec, Brazil) up to 1.50 wt% were investigated together with LiF-free Al_2O_3–4 wt%Nb_2O_5, for control. All ceramic compositions were sintered at 1300, 1350 and 1400 °C for 3 h under a pressure of 50 MPa. The measurement of elastic properties was performed by the impulse excitation technique, using samples of 57 mm diameter with 60 g of mass. They were measured in a Sonelastic[®] equipment, from ATCP Engenharia, Brazil. For the Vickers microhardness, with 1 kgf application load for 15 s, using 20 mm diameter and 5 g specimens, tests were carried out in a model Micromet 5104 Buehler equipment. The samples used for the ballistic test to evaluate residual velocity were the same of the elastic properties analysis, fixed as shown in Fig. 1a. The multilayered armor system (MAS), studied in the present work (Fig. 1b) is composed of a hexagonal (3.8 cm edge) ceramic front, followed by a single layer of aramid fabric to assist in containing the fragments. This second layer of aramid (Kevlar[TM], from LFJ Blindagens, Brazil), was composed of 18 plies with areal density of 0.460 kg/m^2, bonded with neoprene. A back layer of a 5052 H34 aluminum alloy is placed behind the aramid fabric layer, illustrated in Fig. 1b.

The residual velocity tests were performed as per ABNT NBR 15 000 [31], with commercial 7.62 mm M1 ammunition shot 15 m from the target. The ballistic tests of indentation in the modeling clay witness were performed following the NIJ-0101.06 [31] body armor standard, to evaluate the protection level of the MAS. In this test, the MAS target, fixed in front of the clay witness (applied to simulate the consistency of the human body), were also 15 m away from the shooting gun barrel. The projectile's velocity measuring device was a model B290 High Pressure Instrumentation (HPI) equipment. The ballistic tests were performed in the Brazilian Army Assessment Center ("Centro de Avaliações do Exército" – CAEx), Rio de Janeiro, Brazil. The fracture surfaces of the ceramic targets were observed using scanning electron microscopy (SEM), in a model TM3000 Hitachi equipment, available at the Nuclear Engineering Institute (IEN), Rio de Janeiro, Brazil.

3. Results and discussion

Fig. 2 presents microhardness results for the investigated ceramics. In this figure, for each sintering temperature, the addition of LiF causes a higher microhardness as compared to the corresponding one for the control LiF-free Al_2O_3–4 wt%Nb_2O_5. A tendency for superior values of microhardness at 1400 °C is observed in Fig. 2, in comparison with ceramics sintered at 1300 and 1350 °C. This is an expected result, since higher sintering temperatures promote better structure consolidation, which is associated with improved
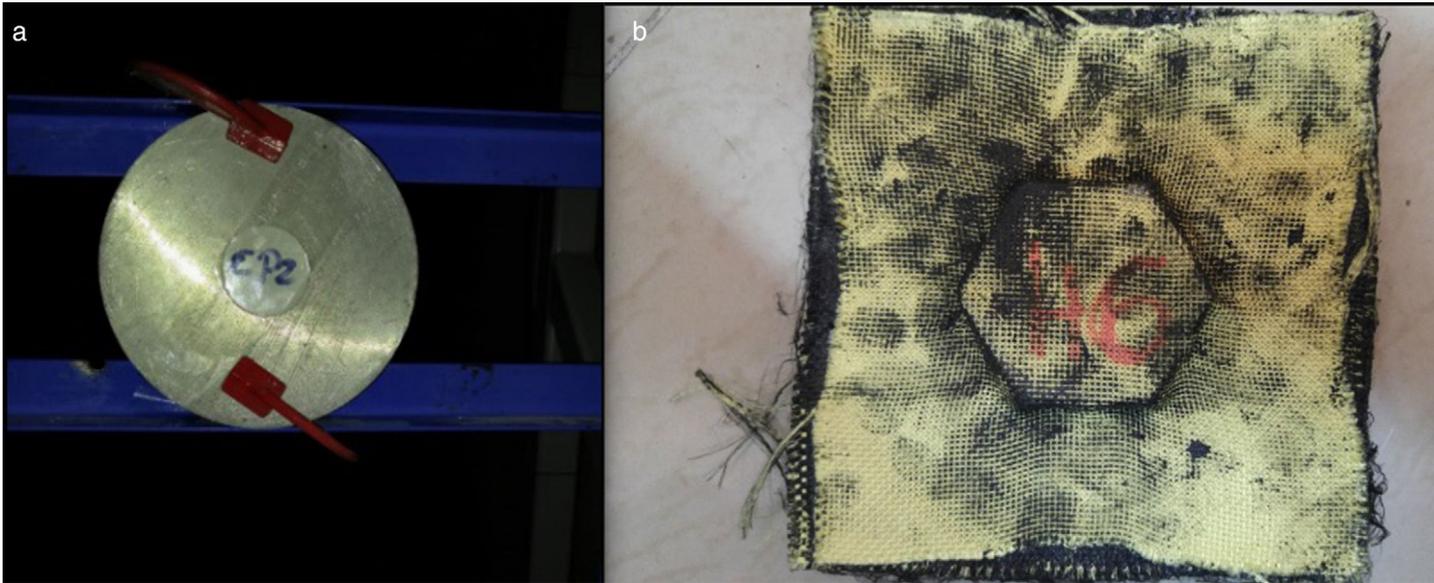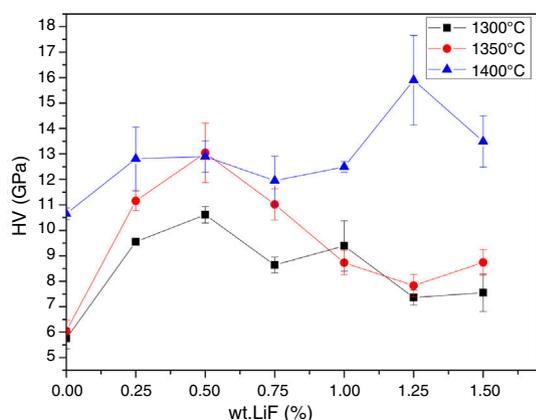
Fig. 1 – Fixation of the samples for the ballistic tests of (a) residual velocity and (b) plasticine indentation.

Fig. 2 – Vickers microhardness *vs.* composition for the different temperatures.

mechanical properties [32]. It is also important to notice in Fig. 2 that a maximum in microhardness is reached for 0.5 wt% LiF at both 1300 and 1350 °C sintering temperatures. Due to the densification and microhardness values obtained for the LiF addition of 0.5 wt%, it was considered that this was the optimized composition. Indeed, the densification of the investigated ceramic compositions was previously studied and presented elsewhere [14]. It was then found best results for the 0.5 wt% addition of LiF. Therefore, the Al_2O_3–4 wt%Nb_2O_5–0.5 wt%LiF had its properties and behavior analyzed in comparison with the control Al_2O_3–4 wt%Nb_2O_5, as reference material.

Table 1 shows the elastic properties: Young and shear moduli as well as Poisson coefficient, and Lamé constant of the sintered samples. At the temperature of 1300 °C, samples with LiF addition obtained elastic and shear moduli comparable to those reported in the literature [19], in plain Al_2O_3–4 wt%Nb_2O_5 at the sintering temperature of 1400 °C. Samples containing LiF sintered at 1350 °C disclosed Young and shear moduli comparable to those obtained by Trindade et al. [19] without the addition of LiF and sintering temperature of 1400 °C for 8 h. In practice, such small difference is fully justified in terms of the reduction of MAS ceramic component production cost. This indicates that the addition of 0.5 wt% LiF allowed a reduction of 100 °C in the sintering
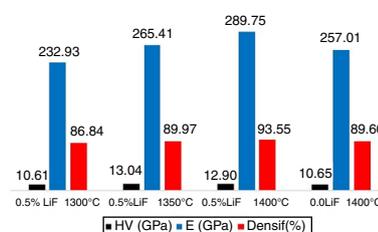
Fig. 3 – Comparison between the microhardness, Young modulus and the densification values.

Table 3 – Mean values of impact and residual velocities and absorbed energy.			
Samples [Al_2O_3–4%Nb_2O_5]–nLiF	V_i (m/s)	V_R (m/s)	E_{abs} (%)
0.5%LiF – 1300 °C	848.99	726.66	26.71 ± 3.40
0.5%LiF – 1350 °C	845.35	722.48	26.87 ± 5.07
0.5%LiF – 1400 °C	848.58	704.60	30.75 ± 9.06
0.0%LiF – 1400 °C	844.17	711.01	28.96 ± 6.54

temperature, without causing a significant reduction of the elastic properties.

From the elastic properties, the velocities of the elastic waves (C_0) of the samples could be determined. Table 2 shows the velocities of elastic waves acting on the samples used in the ballistic test. The C_0 values for samples with 0.5 wt% LiF sintered at 1300 °C, and those without the additive and sintered at 1400 °C, exhibited a relative small discrepancy of the order of 3%. This small reduction is fully rewarded by the significant reduction in sintering temperature (100 °C) in terms of performance and cost. The graph of Fig. 3 shows a comparison between the values of microhardness and modulus of elasticity obtained, and the densification of samples without LiF and with 0.5 wt% of this additive [14], in the three temperatures studied.

The results of the absorbed energy by the distinct ceramic components subjected to the ballistic impact are presented in Table 3. Comparatively, it was observed that the energy absorbed by the ceramics without the addition of LiF at 1400 °C was close to that obtained with the LiF addition sintered at 1300 °C. Therefore, the inclusion of LiF contributed to improve the energy absorption of the ceramic,

Table 1 – Elastic properties of the samples used in the ballistic tests.				
Samples [Al_2O_3–4%Nb_2O_5]–nLiF	E (GPa)	G (GPa)	ν	λ (GPa)
0.5%LiF – 1300 °C	232.935 ± 5.052	93.90 ± 2.08	0.24	86.90 ± 1.59
0.5%LiF – 1350 °C	265.414 ± 4.630	106.99 ± 1.89	0.24	99.03 ± 1.61
0.5%LiF – 1400 °C	289.754 ± 4.908	116.81 ± 1.99	0.24	108.11 ± 1.87
0.0%LiF – 1400 °C	257.010 ± 20.093	103.61 ± 8.13	0.24	95.87 ± 7.22

Table 2 – Elastic waves velocities of the samples used in the ballistic tests.				
Samples [Al_2O_3–4%Nb_2O_5]–nLiF	C_0 (km/s)	C_R (km/s)	C_L (km/s)	C_S (km/s)
0.5%LiF – 1300 °C	8.19 ± 0.09	7.16 ± 0.08	8.90 ± 0.10	5.20 ± 0.06
0.5%LiF – 1350 °C	8.52 ± 0.09	7.44 ± 0.07	9.26 ± 0.08	5.41 ± 0.05
0.5%LiF – 1400 °C	8.81 ± 0.07	7.69 ± 0.06	9.57 ± 0.08	5.59 ± 0.05
0.0%LiF – 1400 °C	8.47 ± 0.22	7.40 ± 0.19	9.20 ± 0.24	5.38 ± 0.14
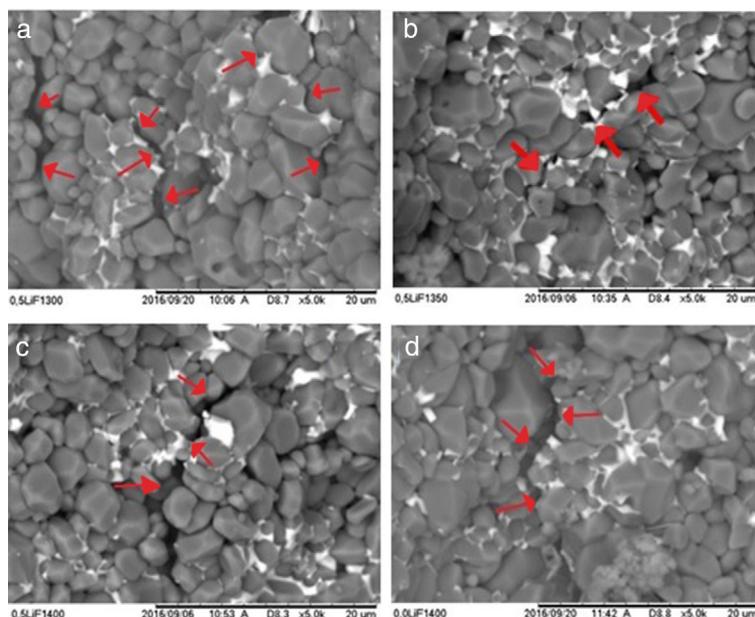
Fig. 4 – SEM micrograph of crack propagation in samples: with 0.5% LiF sintered at (a) 1300 °C, (b) 1350 °C, (c) 1400 °C, and (d) without LiF sintered at 1400 °C.

Table 4 – Mean values of indentation in the clay witness.

Samples [Al_2O_3–4%Nb_2O_5]–nLiF	V_i (m/s)	Penetration (mm)
0.5%LiF – 1300 °C	846.75	37.20 ± 0.89
0.5%LiF – 1350 °C	842.72	37.44 ± 1.11
0.5%LiF – 1400 °C	848.47	34.16 ± 2.00
0.0%LiF – 1400 °C	847.86	34.52 ± 2.23

even sintering at a temperature 100 °C lower, as compared to the Al_2O_3–4 wt%Nb_2O_5 used in previous works [10,19]. In addition, by analyzing the behavior of the ceramic compound in terms of energy absorption, it is possible to observe that higher values of densification, reported by Santos et al. [14], and modulus of elasticity, Table 1, did not necessarily result in a higher percentage of absorbed energy. There is a marked difference between the sonic impedance of the porosity and the solid part of the ceramic. In fact, a pore acts like a hot spot, accumulating energy [29]. This evidences the role of porosity as an important parameter in the absorption of energy. A feature of a ceramic, which performs well for energy absorption, is the intergranular propagation of cracks. SEM micrographs showed in Fig. 4 that fractured samples after ballistic impacts revealed such behavior, reinforcing the results of Table 4.

Table 4 presents the results of indentation (trauma) in the witness clay. All compositions met the requirement of the standard [30], with trauma less than 44 mm. The trauma left in the witness clay in the ceramic with 0.5 wt% LiF sintered at 1300 °C was only 7% greater than that produced using the control ceramic without the addition of LiF sintered at 1400 °C. This confirms the efficiency of the new LiF-added ceramic compound studied and suggests it to be applied as a novel ceramic component in MAS, sintered at lower temperatures, 1300 °C, which saves time and processing energy.

4.   Conclusions

- All additions of LiF increased the microhardness of the Al_2O_3–4 wt%Nb_2O_5 ceramics, especially the addition of 0.5 wt%, associated with maximum values at 1300 and 1350 °C.
- The results obtained from the mechanical properties of the ceramic composition with LiF, sintered at different temperatures, showed that it is possible to reduce the sintering temperature by 100 °C (from 1400 to 1300 °C) without significant reduction in the elastic properties.
- High Young's modulus, hardness and densification (low porosity) do not necessarily represent a more efficient ballistic armor. This evidences the role played by the porosity and bond force roles in ballistic impact energy absorption.
- The results of the ballistic tests also indicated an amazing performance of the new ceramic composite, even sintered at lower temperatures.
- By the significant decrease in the sintering temperature, there is a corresponding reduction in the processing cost of the material presented in this work, which showed interesting results for potential ballistic application, as in MAS.

Conflicts of interest

The authors declare no conflicts of interest.

Acknowledgements

REFERENCES

[1] Zang W, Guo F, Liu J, Du H, Hou F, et al. Lightweight alumina based fibrous ceramics with different high temperature binder. Ceram Intern 2016;42:10310–6.

[2] Hassan AM, Awaad M, Bondioli F. Densification behavior and mechanical properties of niobium-oxide-doped alumina ceramics. J Ceram Sci Technol 2014;5:51–6.

[3] Liu Y, Min F, Zhu J, Zhang M. Effect of nanometer Al_2O_3 powder on microstructure and properties of alumina ceramics by microwave sintering. Mater Sci Eng A 2012;546:328–31.

[4] Zhu B, Zhu Y, Li X, Zhao F. Effect of ceramic bonding phases on the thermo-mechanical properties of Al_2O_3–C refractories. Ceram Intern 2013;39:6069–76.

[5] Zawrah MF, Khattab RM, Girgis LG, et al. Effect of CTAB as a foaming agent on the properties of alumina ceramic membranes. Ceram Intern 2014;40:5299–305.

[6] Nevarez-Rascon A, González-Lopez A, Acosta-Torres LS, Nevarez-Rascon MM, Orrantia-Borunda E. Synthesis, biocompatibility and mechanical properties of ZrO_2–Al_2O_3 ceramics composites. Dent Mater J 2016;35:392–8.

[7] Ai YL, Jiang N, He F, Liang BL, He W. Mechanical properties of La_2O_3 and Nb_2O_5 doped Al_2O_3 ceramics prepared by microwave sintering. Key Eng Mater 2013;544:281–5.

[8] Lima ES, Santos APO, Itaboray LM, Santos C, Cabral RF. Development and characterization of the Al_2O_3–YAG ceramic composites. Mater Sci Forum 2014;798–799:383–5.

[9] Liu H, Liu H, Huang C, Zou B, Chai Y. Effects of MgO and Y_2O_3 on the microstructure and mechanical properties of Al_2O_3 ceramics. Key Eng Mater 2013;589–590:572–7.

[10] Gomes AV, Louro LHL, Costa CRC. Ballistic behavior of alumina with niobia additions. J Phys IV France 2006;134:1009–14.

[11] Sposito L, Piancastelli A, Martelli S. Production and characterization of transparent $MgAl_2O_4$ prepared by hot pressing. J Eur Ceram Soc 2013;33:737–47.

[12] Sutorik AC, Gilde G, Cooper C, Wright J, Hilton C. The effect of varied amounts of LiF sintering aid on the transparency of alumina rich spinel ceramic with the composition $MgO \cdot 1.5Al_2O_3$. J Am Ceram Soc 2012;95:1807–10.

[13] Reimanis I, Kleebe H-J. A review on the sintering and microstructure development of transparent spinel ($MgAl_2O_4$). J Am Ceram Soc 2009;92:1472–80.

[14] Santos JL, Marçal RLSB, Jesus PRR, Gomes AV, Lima EP Jr, Monteiro SN, de Campos JB, Louro LHL. Effect of LiF as sintering agent on the densification and phase formation in Al_2O_3–4wt%Nb_2O_5 ceramic compound. Metall Mater Trans A 2017;48(10):4432–40.

[15] Medvedovski E. Ballistic performance of armour ceramics. Part 1 and 2. Ceram Int 2010;36:2103–27.

[16] Shokrieh MM, Javadpour GH. Penetration analysis of a projectile in ceramic composite armor. Compos Struct 2008;82:269–76.

[17] Medvedovski E. Lightweight ceramic composite armour system. Adv Appl Ceram 2006;105:241–5.

[18] James B. Practical issues in ceramic armor design. In: McCauley JW, Crowson A, Gooch WA Jr, Rajendran AM, Bless SJ, Logan K, et al, editors. Ceramic armor material by design: ceramic transactions, vol. 134. New Jersey, USA: John Wiley & Sons; 2012. p. 33–44.

[19] Trindade W, Prado da Silva MH, Gomes AV, de Campos JB, Louro LHL. Processing and properties of niobia-doped alumina sintered at 1400 °C. Mater Sci Forum 2014;798–799:665–70.

[20] Assis FS, Pereira AC, Garcia Filho FC, Lima EP Jr, Monteiro SN, Weber RP. Performance of jute non-woven mat reinforced polyester matrix composites in multilayered armor. J Mater Res Technol 2018, http://dx.doi.org/10.1016/j.jmrt.2018.05.026 [in press].

[21] Braga FO, Milanezi TL, Monteiro SN, Louro LHL, Gomes AV, Lima EP Jr. Ballistic comparison between epoxy-ramie and epoxy-aramid composites in multilayered armor systems. J Mater Res Technol 2018, http://dx.doi.org/10.1016/j.jmrt.2018.06.018 [in press].

[22] Braga FO, Luz FS, Monteiro SN, Lima EP Jr. Effect of the impact geometry in the ballisitic trauma absorption of a ceramic multilayered armor system. J Mater Res Technol 2018, http://dx.doi.org/10.1016/j.jmrt.2018.06.019 [in press].

[23] Monteiro SN, Braga FO, Lima EP Jr, Louro LHL, Drelich JW. Promising curaua fiber-reinforced polyester composite for high impact ballisitic multilayered armor. Polym Eng Sci 2017;57:947–54.

[24] Monteiro SN, Candido VS, Braga FO, Bolzan LT, Weber RP, Drelich JW. Sugarcane bagasse waste in composites for multilayered armor. Eur Polym J 2016;78: 173–85.

[25] Monteiro SN, Milanezi TL, Louro LHL, Lima EP Jr, Braga FO, Gomes AV, et al. Novel ballistic ramie fabric composite competing with Kevlar™ fabric in multilayered armor. Mater Des 2016;96:263–9.

[26] Monteiro SN, Louro LHL, Trindade W, Elias CN, Ferreira CL, Lima ES, et al. Natural curaua fiber-reinforced composites in multilayered ballistic armor. Metall Mater Trans A 2015;46(10):4567–77.

[27] Monteiro SN, Lima EP Jr, Louro LHL, Silva LC, Drelich JW. Unlocking function of aramid fibers in multilayered ballistic armor. Metall Mater Trans A 2015;46:37–9.

[28] Luz FS, Lima EP Jr, Louro LHL, Monteiro SN. Ballistic test of multilayered armor with intermediate epoxy composite reinforced with jute fabric. Mater Res 2015;18: 170–7.

[29] Meyers MA. Dynamic behavior of materials. New York, USA: John Wiley & Sons; 1994.

[30] NIJ Standard 0101.06. Ballistic resistance of personal body armor. U.S. Department of Justice/Office of Justice Programs; 2008.

[31] Brazilian Association of Technical Norms, ABNT NBR 15000. Armor for ballistic impacts – classification and evaluation criteria. Rio de Janeiro, Brazil; 2005 [in Portuguese].

[32] Watchman JB, Cannon WR, Mathewson MJ. Mechanical properties of ceramics. 2nd ed. Hoboken, NJ, USA: John Wiley & Sons; 2009.